Characterization of the impact of ethanol on the formation of soot particles in gasoline turbulent diffusion flames

Hong-Quan Do, Eric Therssen, Kanika Sood, Lucia Giarracca-Mehl, Benoîte Lefort, Luc-Sy Tran, Xavier Mercier

Characterization of the impact of ethanol on the formation of soot particles in gasoline turbulent diffusion flames

Hong-Quan Do[a,b*], Eric Therssen[a], Kanika Sood[a], Lucia Giarracca-Mehl[c], Benoîte Lefort[b], Luc-Sy Tran[a], Xavier Mercier[a]

[a]*Univ. Lille, CNRS, UMR 8522 - PC2A - Physicochimie des Processus de Combustion et de l'Atmosphère, F-59000 Lille, France*

[b]*Université de Bourgogne, DRIVE Lab, 49 rue Mademoiselle Bourgeois, 58000 Nevers, France*

[c] *IFP Energies nouvelles, Institut Carnot IFPEN Transports Energie, 1 et 4 avenue de Bois-Préau, 92852 Rueil-Malmaison, France*

Abstract

The objective of this study was to characterize the impact of ethanol as a fuel additive on soot formation in turbulent diffusion flames of different gasoline mixtures with varying alcohol concentrations. A TRF mixture (Toluene Reference Fuel), defined as a surrogate representative of standard gasolines of type SP95, was used as the reference fuel. The experimental results obtained in this study offer important observations regarding the impact of ethanol on soot formation and provide useful data for accurate CFD prediction. 11 flames of TRF mixed with various ethanol mole fractions from 0 to 100% were studied by using two complementary approaches, keeping either the flame power (FPW) or the mass flow rate (MFR) constant. The soot volume fraction (f_v) was measured by laser induced incandescence (LII). Absolute f_v values were obtained by an auto-calibrated method requiring a radiation source of known luminescence to calibrate the detection system. Laser induced fluorescence (LIF) was also used to measure important soot precursors, i.e. polycyclic aromatic hydrocarbons (PAHs). The experimental results highlighted a quasi-linear reduction in soot formation with increasing substituted volume fraction of ethanol until 40%, above which the linear relation was not followed. The soot particles completely disappeared in the pure ethanol and TRF-E85* flame in the case of constant FPW and constant MFR respectively. These results also highlighted a stronger inhibiting effect of ethanol on soot formation with respect to subsequent ethanol substitution at constant MFR, characterized by a gradual decrease in the flame height. Experiments with commercial gasoline SP95-E10 and E85 were also carried out for the first time for soot formation under turbulent conditions. The measured f_v and PAHs profiles illustrated that the used TRF is indeed an appropriate gasoline surrogate for studies aiming at characterizing soot formation.

Keywords: Ethanol, Surrogate gasoline, Soot formation, Polycyclic aromatic hydrocarbon, Turbulent diffusion flame

---

*Corresponding author. Email-address:

Hong-Quan.Do@u-bourgogne.fr

Information for Colloquium Chairs and Cochairs, Editors, and Reviewers

1) Novelty and Significance Statement

This study presents the significant effect of ethanol substitution in soot reduction in turbulent diffusion flames of gasoline surrogate and commercial gasoline. The novelty lies in the unexplored transient zone amidst fundamental and applied studies, characterized for instance by turbulent flames chosen to perform these experiments. Though essential for kinetic analysis and accurate CFD prediction, experimental data in this zone is rather limited. Ethanol amount is varied from 0 to 100% (constant FPW or constant MFR). Established by our experimental set-up, about 60-80% ethanol substitution in gasoline is sufficient to lead to ~100% soot reduction. This observation is related to the chemical and dilution effect of ethanol. Furthermore, soot reduction efficiency appears to be stronger in the turbulent than in the laminar regime suggesting that the phenomenon of turbulence itself also plays a role. These findings can be of use to car manufacturers to develop low-soot direct injection spark-ignition engines.

2) Author Contributions

- HQD: Performed research, Analyzed data, Wrote the original draft, Reviewed and Edited the paper
- ET: Supervision, Analyzed data, Reviewed and Edited the paper
- KS: Analyzed data, Reviewed and Edited the paper
- LGM: Analyzed data, Reviewed and Edited the paper
- BL: Wrote the original draft, Reviewed and Edited the paper
- LST: Analyzed data, Wrote the original draft, Reviewed and Edited the paper
- XM: Supervision, Analyzed data, Wrote the original draft, Reviewed and Edited the paper

3) Authors' Preference and Justification for Mode of Presentation at the Symposium

The authors prefer **OPP** presentation at the Symposium, for the following reasons:

- A unique and noteworthy impact of ethanol substitution in turbulent diffusion sooting flame of gasoline surrogate.
- The chemical and dilution effects of ethanol on soot reduction have been experimentally proved.
- The similar PAHs and soot profiles have been observed between commercial bio-gasolines and their surrogates.
- Our findings help car manufacturers develop low-soot direct injection spark ignition engine.

1. Introduction

Although the share of electric vehicles will keep growing, the demand for gasoline and diesel to power the existing fleet of vehicles will remain substantial. The is also true for the foreseeable future, as the engines of heavy-duty vehicles, ships and planes will continue to rely on liquid fuels because of their high energy density [1]. Bio-ethanol is an attractive alternative fuel with a high octane number (RON/MON = 120/99) for spark-ignited internal combustion engines [2]. Studies have shown that adding ethanol to the fuel reduces particulate matter emissions in gasoline direct injection engines [3]. To investigate the chemical effect of ethanol on soot formation, laboratory scale flames enable to limit the effect of different engine operating parameters. Laminar diffusion flames of gasoline were extensively employed for this purpose [4–7].

Since the composition of gasoline is very complex, a TRF mixture containing iso-octane, toluene and n-heptane has been widely used as a suitable gasoline surrogate to investigate the chemical kinetic impact of ethanol on soot formation [7–12]. The dilution effects of ethanol results in lower toluene concentration in the fuel stream of TRF mixture, which in turn lowers the rates of formation of aromatic soot precursors in laminar diffusion flames of TRF [7]. Hua et *al.* [10] have developed a kinetic model to elucidate the influence of ethanol on soot formation in laminar diffusion sooting flame of TRF, explaining that ethanol can provide OH groups, which may enhance the oxidation of PAHs and soot particles, ultimately leading to lower soot concentration. Currently, most of the studies in the literature have either focused on fundamental laboratory scale reactors [13] or application based internal combustion engines to investigate the impact of ethanol on soot formation during the combustion of gasoline or its surrogates. However, experimental studies focusing on the transient zone located between the fundamental reactors and the internal combustion engines are very limited. Turbulent flames are deemed suitable to characterize this transient zone. We noted that so far, only one experimental study by Lemaire et *al.* [12] has focused on the impact of ethanol on the formation of soot particles in turbulent sooting flames. However, experimental data obtained in their study are not easily applicable for the development of CFD modeling due to the complexity of the burner configuration.

Hence, the present study aims to address the gap of this transitory zone by not only providing valuable experimental data for accurate CFD prediction, but also offering interesting and important observations regarding the impact of ethanol on soot formation in the combustion of gasoline or its surrogates. To do so, 11 jet spray flames of TRF mixed with various ethanol fractions from 0 to 100% were studied for the first time by using a combined approach, keeping either the flame power (FPW) or the mass flow rate (MFR) constant. These two parameters are very important for the combustion of liquid fuels, but it was not possible to keep both constant in our flame conditions. The FPW dictates the engine power and the thermal engine yield while the MFR directly impacts the atomization efficiency of jet spray, and then the fuel evaporation. The soot volume fraction (f_v) was measured using auto-calibrated laser induced incandescence (LII). The relative concentration of PAHs in the flames was measured using the LIF technique. The temperature profiles of the flames were measured by a thermocouple. Furthermore, we also highlighted for the first time the excellent mimicry of the SP95-E10 and E85 commercial gasoline by the TRF-Ethanol mixtures in terms of their soot formation tendencies.

2. Experiment methods

2.1. Burner and flame conditions

The turbulent spray flames were stabilized on a homemade burner as presented in Fig. S1 consisting of a nebulizer (DIHEN-170-AA) [14] for liquid fuel's atomization and an oxidation air stabilization system. In this study, nitrogen was used as the nebulized gas. The air flow was injected under a honeycomb structure which allowed a better stabilization of the flame. The nebulizer was placed in the center of the honeycomb structure. For all studied flames, the flow rates of N_2 and Air were kept constant at 0.25 Ln/min and 19.6 Ln/min respectively. The flame conditions for the 11 TRF-Ethanol flames are reported in Table 1. The studied mixtures were prepared by mixing 4 pure chemical compounds: iso-octane, toluene, n-heptane and ethanol. The intended composition of the fuel mixtures prepared was also verified using gas chromatography (GC). The uncertainty associated with the mole fractions of each of the fuel components was determined to be less than 3% as presented in Table S1.

2.2. Experimental setup

2.2.1. Flame temperature measurement

The vertical centerline temperature profiles of the studied flames were measured with a type S thermocouple (TC S.A., Pt-Pt/10%Rh) having 0.35 mm wire diameter and 1.01 mm bead diameter. The thermocouple was radially introduced and remained in flame for 5 seconds, then cleaned by placing it in the blue zone of the flame after every measurement in the sooting zone. The thermocouple temperature measurements were corrected from the radiation losses based on extrapolation to zero wire diameter as employed in Elias et *al.* [15]. The uncertainty on the temperature was estimated to be around ± 100 K.

2.2.2. Determination of soot volume fraction profiles

Soot volume fraction profiles were determined using laser induced incandescence (LII) carried out by using a laser excitation wavelength at 532 nm, which also allows to measure PAHs relative concentration from the LIF signal with the same set-up. The laser beam passed through a pinhole to provide a top-hat irradiance profile at the position of the LII measurement in the flame as presented in Fig. S2(l). The LII signal was collected at a right angle from the laser axis by a system of two cylindrical lenses (f_1 = 400 mm and f_2 = 200 mm) associated with a spectrometer Acton SP300i. A diffraction grating 150 groves/mm, blazed at 800 nm (high transmission in near IR) was used. The center wavelength of the diffraction grating was set at 750 nm allowing to collect the emission spectral range from 609 nm to 890 nm. The LII signals were collected using a XP2020Q photomultiplier to determine the fluence curves and identify the laser fluence used for the LII experiments. Additionally, 1D spectral images of the LII signals were also collected by a Roper PIMAX4 ICCD camera which were used to determine the soot volume fractions.

Table 1. Flame conditions for the two experimental series. *Serie 1*: same flame power (FPW). *Serie 2*: same mass flow rate of fuel (MFR). $x_{\text{iso-octane}}$, x_{toluene}, $x_{\text{n-heptane}}$, x_{ethanol} are the mole fractions of iso-octane, toluene, n-heptane and ethanol in the fuel mixture, respectively. The number in the flame name corresponds to the % volume of ethanol in the TRF mixture. The Reynolds numbers of nitrogen nebulized gas (Re_{N2}) at 298 K and 1 atm = (Velocity of nitrogen nebulized gas flow × Gas orifice internal diameter) / Kinematic viscosity of nitrogen.

	Flame name					
Serie 1: Same FPW	**TRF**	**TRF-E10**	**TRF-E22**	**TRF-39**	**TRF-E85**	**E100**
FPW (kJ/h)	4.24	4.24	4.24	4.24	4.24	4.24
MFR (g/h)	98.2	102.1	107.6	115.8	145.2	158.1
Serie 2: Same MFR	**TRF**	**TRF-E10***	**TRF-E22***	**TRF-E39***	**TRF-E85***	**E100***
FPW (kJ/h)	4.24	4.08	3.87	3.59	2.86	2.63
MFR (g/h)	98.2	98.2	98.2	98.2	98.2	98.2
For two series						
$x_{\text{iso-octane}}$	0.447	0.358	0.268	0.179	0.031	0.000
x_{toluene}	0.423	0.338	0.254	0.169	0.029	0.000
$x_{\text{n-heptane}}$	0.130	0.104	0.078	0.052	0.009	0.000
x_{ethanol}	0.000	0.200	0.400	0.600	0.931	1.000
Flowrate of N_2 (Ln/min)	0.25	0.25	0.25	0.25	0.25	0.25
Flowrate of Air (Ln/min)	19.6	19.6	19.6	19.6	19.6	19.6
Re_{N2} at 298 K and 1 atm	4875	4875	4875	4875	4875	4875

A Notch filter centered at 532 ± 9.8 nm was positioned just before the spectrometer to remove the intense Rayleigh laser scattering. All the recorded LII signals were measured using a laser fluence below the soot sublimation threshold energy, as determined from the experimental fluence curves presented in Fig. S2 to minimize the influence of soot particle temperature on the measured LII signal [16]. Based on these considerations, a laser fluence of 54 mJ/cm^2 was considered suitable for the nine most sooting flames: TRF, TRF-E10, TRF-E22, TRF-E39, TRF-E10*, TRF-E-22*, TRF-E39*, E10, E10*. This value is the best compromise we found to allow the measurements of the LII signal without being blurred by the visible LIF signal. We used a laser fluence of 108 mJ/cm^2 for the six slightly and non-sooting flames: TRF-E85, Ethanol, TRF-E85*, Ethanol*, E85, E85* to improve the signal to noise ratio of LII measurement. The LII signal from the soot particles was measured with the detection system characterized by the solid angle of collection Ω and the transmission coefficient of the whole collection system β. Thus, the detected LII signal S_{LII} (T_p, λ) can be expressed as:

$$S_{LII}(T_p,\lambda) = \frac{12\pi hc^2 E_m(\lambda)}{\lambda^6} \cdot \frac{1}{\exp\left(\frac{hc}{\lambda k_B T_p}\right) - 1} \cdot V_m \cdot \Omega \cdot \beta \cdot \Delta\lambda \cdot f_v \qquad (1)$$

where λ is the emission wavelength, k_b is the Boltzmann constant, c is the light speed, h is the Planck constant, T_p is the average temperature of soot particles determined on the LII spectrum, $\Delta\lambda$ is the emission spectral range, V_m is the measurement volume, f_v is the soot volume fraction. To obtain absolute f_v values from the LII signal, we calibrated the detection system using an auto-calibrated method requiring a radiation source of known luminescence to determine the measurement volume V_m and the term $\Omega \cdot \beta$. The LII signal for f_v determination in this study was collected with the spectrometer at 800 nm.

$E_m(\lambda)$ has been determined along the vertical centerline of the flame using the low laser fluence methodology [17] using the following expression:

$$E_m(\lambda) = \frac{(T_p - T_g) \cdot \lambda_{laser} \cdot \rho_s \cdot c_s}{6\pi \cdot F} \qquad (2)$$

where T_g is the temperature of flame, λ_{laser} is the laser wavelength, F is the laser fluence, ρ_c is the density of soot particles and c_s is the specific heat of soot particles which was considered constant, i.e. 2.3 J·g^{-}

$^{1}\cdot K^{-1}$ [18]. The density of soot ρ_c in the sooting flame was linearly extrapolated along the centerline of the flame, ranging from 1.3 g/cm^3 for nascent soot to 1.8 g/cm^3 for mature soot [17]. The evolution of $E_m(\lambda)$ with respect to the flame height for all sooting flames is presented in Fig. S3. The uncertainty of f_v was estimated to be around ± 30% based on the uncertainties of all parameters in the Eq 1 and the uncertainties in the mixture preparation.

2.2.3. Soot precursors characterization

Soot precursors including polycyclic aromatic hydrocarbons (PAHs) were measured by laser induced fluorescence (LIF) using a laser excitation wavelength at 532 nm. All the recorded LIF signals have been measured using a laser fluence below the LII threshold which was defined at 14.4 mJ/cm^2. The LIF signal was collected using the same detection system as for the LII measurements. The center wavelength of the diffraction grating was set at 500 nm allowing to collect the LIF signal in the spectral range from 358 nm to 641 nm. In this study, 500 single-shots were collected and averaged for both LII and LIF experiments. LIF and LII signal have been corrected from the natural flame emission which was systematically subtracted from the measured signals at every 1 cm of flame height.

3. Results and discussions

3.1. Impact of ethanol on soot formation in TRF flame

Before investigating the impact of ethanol on soot formation in the TRF flame, it is important to discuss the TRF flame structure. Fig. 1 illustrates the evolution of LIF, LII normalized signal and flame temperature with respect to the height above burner (HAB) along the centerline of the TRF flame. As seen in this figure, a bimodal profile of the LIF signal corresponding to the formation of PAHs species is obtained in TRF flame. The LIF signal starts at 0 mm due to presence of petrogenic aromatics in the fuel mixture, then increases strongly up to 20 mm due to the expansion of the liquid jet. Afterwards, it sharply decreases until 70 mm before rising once more. The consumption of fuel leads to the decrease of LIF and a buildup of new species such as pyrogenic PAHs, which fluoresce at 532 nm excitation. Thus, the second peak of LIF profile was obtained at 110 mm. The pyrogenic PAH species are the ones formed during combustion. The term "pyrogenic" is used here to distinguish with aromatics already present in the fuels (toluene in TRF fuels, and PAHs and other aromatics in real fuels presented in Section 3.3). The pyrogenic PAHs are considered as soot precursors. However, the LIF signal of the first mode is higher by a factor 3 than that of the second mode. Hence, to better apprehend the impact of ethanol on soot formation, we focus exclusively on the second mode zone (starting from 70 mm) for PAHs species in the following section. As can be seen in Fig. 1, the flame temperature at 70 mm is 1570 K, at which the fuel mixture is completely consumed. However, we observed that the signal LIF at 70 mm is not zero, which is attributed to the formation of pyrogenic PAHs appearing before this height. The incandescence from particles starts at 70 mm and reaches its maximum at 130 mm. After this height, the LII signal decreases with increasing of the HAB due to the oxidation processes of soot particles. The maximum temperature of TRF flame is around 1930 K at 130 mm which corresponds to the maximum value of soot volume fraction.

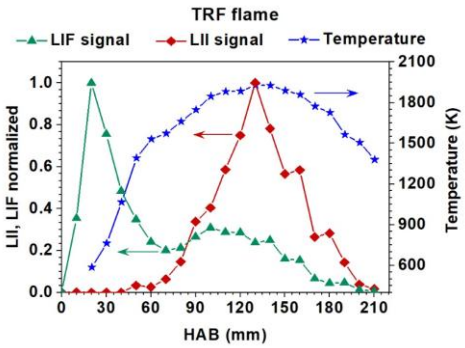

Fig. 1. LII, LIF normalized profiles and the temperature profile measured at the center line of TRF flame.

3.1.1. Constant FPW

Fig. 2 presents a real view of flames (a), 2D-images of LII (b) and of soot precursors from LIF (c) for the 6 TRF-Ethanol flames in the case of constant FPW. The parameters of the camera to take the flame pictures in Fig. 2a were kept identical. The orange color of the flame is mainly due to the thermal radiation from soot particles. When the quantity of ethanol in the mixture increases, the flame height increases while the orange luminosity decreases and even disappears completely in the 100% ethanol flame. The 2D images of the LII and LIF signal rebuilt from the 1D spectral measurements carried out in the 6 flames are reported in Fig. 2b and 2c. These figures clearly illustrate the impact of ethanol substitution on fluorescent soot precursors and soot concentrations. The LII and LIF signals decrease progressively as ethanol is substituted in the TRF mixture. These signals were not detected in the flame of pure ethanol.

Fig. 3 shows the impact of ethanol on the temperature, soot volume fraction and pyrogenic PAHs profiles at the centerline of the TRF flame. Ethanol substitution does not significantly influence the maximum temperature in all flames but definitely extends the overall temperature profile to the burnt gas zone. This observation can be explained by the

increase of MFR. The no discernible difference in flame temperatures between the investigated flames allows the comparison of the LIF signal relative intensities as the relative PAHs concentrations with a satisfying confidence. Increasing the MFR decreases the efficiency of fuel atomization leading to a reduction in combustion efficiency [14]. In addition, the viscosity of TRF mixture increases with ethanol substitution in the mixture (Table S4), which also leads to the decrease of fuel atomization. Note that, the temperatures at 20 mm height above the burner are

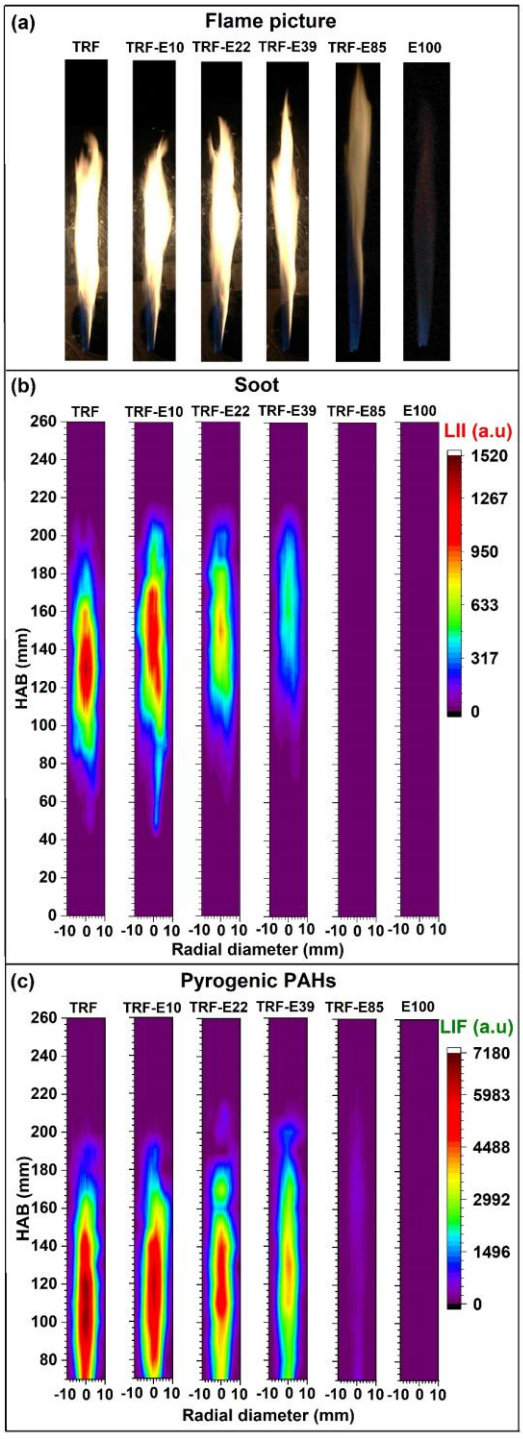

Fig. 2. Flame pictures (a), 2D-images of LII (b) and soot precursors LIF (c) for 6 TRF-Ethanol flames in the case of constant FPW.

around 600 K (see Fig. 3a), ensuring complete fuel evaporation in all flames under investigation, regardless of variations in mixture viscosity. The

carbon mass flow rate of fuel decreases very slightly only 3.3% as can be seen in Table S2 with 100% substitution of ethanol in the mixture. However, we clearly observe a strong reduction of the soot and pyrogenic PAHs indicating the strong chemical and dilution effects of ethanol in inhibiting the formation of soot in the TRF flame. Indeed, the presence of ethanol on TRF mixtures dilutes the concentration of toluene which is an important precursor of pyrogenic PAHs and soot particles. Also, the substitution of ethanol increases the oxygen content in the fuel mixture. The carbon atoms attached to the oxygen atoms are now forming CO_2 instead of soot during the high temperature oxidation as suggested by Westbrook et *al.* [19]. Note that, no 2D f_v data is provided since 2D flame temperature is not available and it is difficult to obtain using thermocouple techniques. The 2D LII and LIF images presented provide the information about the relative distributions of soot and PAHs in the flame. This, combined with profiles of absolute soot volume fraction at the flame centerline, already serves as valuable data for comparison with modeling results.

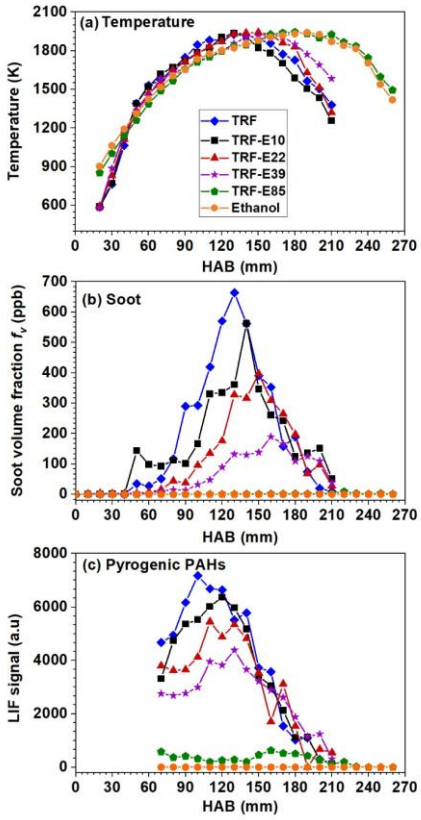

Fig. 3. Temperature profiles, soot volume fraction and pyrogenic PAHs profiles obtained at the centerline of TRF-Ethanol (0-100%) flames in the case of constant FPW.

3.1.2. Constant MFR

Fig. 4 presents a real view of flames (a), 2D-images of LII (b) and of soot precursors from LIF (c) for the 6 TRF-Ethanol flames in the case of constant MFR. As can be seen in Fig. 4a, we observe that the orange luminosity and the flame height decrease with increasing ethanol in the mixture. The orange color disappears completely in the TRF-E85* and E100* flames. This trend of soot reduction was also observed in the 2D-images of LII (Fig. 4b) and soot precursors from LIF (Fig. 4c). The LII and LIF signals were not detected in the TRF-E85* and E100* flames.

Fig. 5 shows the impact of ethanol on the temperature, soot volume fraction and soot precursors profiles at the centerline of the TRF flame (constant MFR). Increasing the ethanol volume in the TRF mixture does not change the maximum temperature in all investigated flames but compresses the temperature profile towards the nebulizer. This observation is due to the constant mass flow rate of fuel mixture leading to a decrease in their FPWs. The reduction in FPW implies a decrease in the flame height. The maximum soot volume fraction and pyrogenic PAHs decreased when ethanol is substituted in the TRF mixture. This approach allows to limit the impact of MFR on soot formation. However, the decrease of carbon mass flow rate (Table S3) was considered in the reduction of soot and PAHs. Thus, the identification of chemical effect of ethanol on soot reduction in this case is more complicated than it was in the case of constant FPW.

3.2. Turbulent combustion of ethanol and soot formation

Fig. 6 shows the reduction of the maximum soot volume fraction and PAHs signal values determined in the flames plotted with respect to the substituted ethanol volume fraction in the TRF mixture. As can be seen in this figure, in both cases (constant MFR or FPW), we observe a quasi-linear reduction of the soot volume fraction in the TRF flame with the volume of ethanol substitution (0 - 40%). Above 40%, this trend is not respected. The impact of ethanol on soot formation is stronger than on PAHs formation and it is easily observed in the case of constant FPW. One of the explanations for this observation could be based on the kinetics of the soot formation process. Indeed, the PAH dimerization is considered an important process for nascent soot formation. Thus, the nascent soot quantity is proportional to the square of PAH concentration at constant temperature and the nascent soot serves as the nucleus for the soot growth process, either by acetylene addition mechanism (HACA) or by condensation of PAH on the surface of soot particles. As can be seen in Fig. 6, 98.6% of soot is reduced in the case of constant FPW in TRF-E85 while 100% of soot reduction is observed for the case of constant MFR. These results

indicate that to reduce soot emissions from gasoline combustion, it is unnecessary to entirely replace gasoline with ethanol. According to our results, adding ethanol in volume fraction ranging within 60-80% is adequate to achieve nearly 100% soot reduction. The impact of ethanol on soot reduction for the case of constant MFR is stronger than that for the case of constant FPW. Indeed, the carbon mass flow rate reduces only 3.3% in the case of constant FPW while it is 40.0% in the case of constant MFR (Table S2 and S3) when ethanol

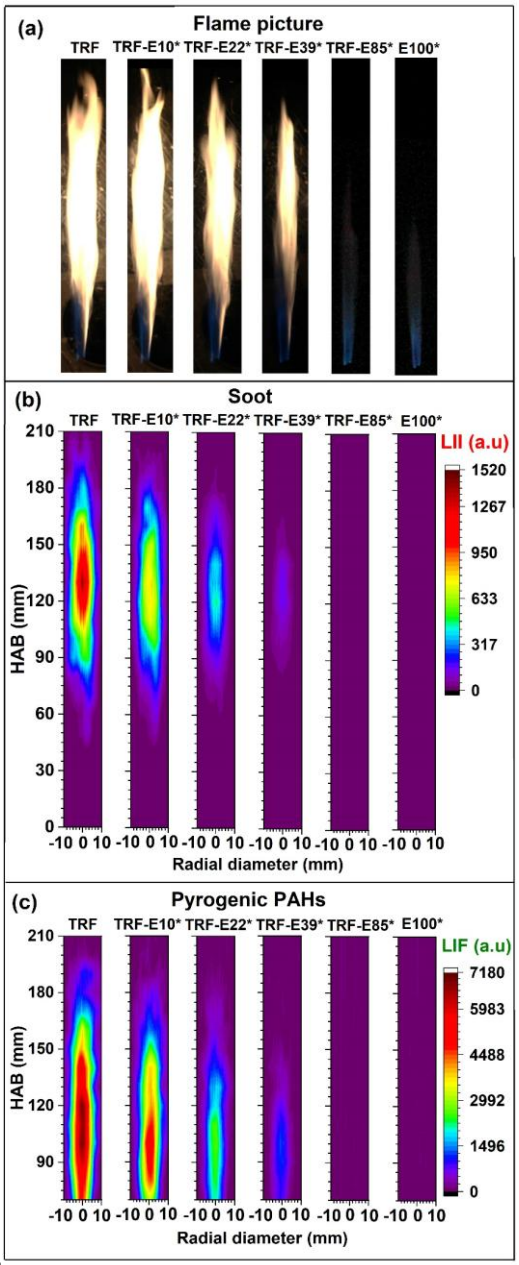

Fig. 4. Picture of flame emission (a), 2D-images of LII (b) and soot precursors LIF (c) for 6 TRF-Ethanol flames in the case of constant MFR

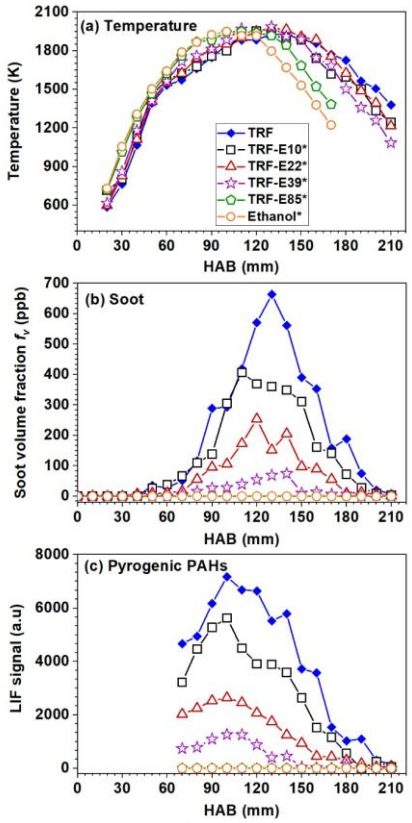

Fig. 5. Temperature profiles, soot volume fraction and pyrogenic PAHs profiles obtained in the centerline of the TRF-Ethanol (0 - 100%) flames with constant MFR.

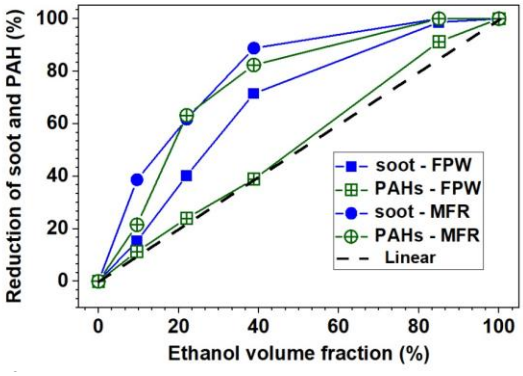

Fig. 6. Reduction of maximum soot volume fraction and pyrogenic PAHs with substituted ethanol volume fraction. FPW: constant flame power, MFR: constant fuel mass flow rate.

is substituted from 0 - 100% in volume in the TRF mixture. Note that the discussion above is solely based on soot volume fraction. Another important

parameter, soot particle number, has not been considered. These two parameters are not always proportional due to their dependence on the soot particle-size distribution (PSD). Recent engine studies in the literature have demonstrated that the influence of added ethanol on the soot particle number is complex and depends strongly on various factors, such as engine operation conditions and ethanol content [20]. Chen et *al.* [21] claimed that high vaporization enthalpy and lower density of ethanol could adversely affect fuel spray break-up and increase soot particle number with increasing ethanol content in gasoline. However, detailed discussions about soot particle number in the studied flames cannot be conducted in the present paper due to the unavailability of PSD data.

Although different burners and configurations were used, as a first approximation, we compared the trend effect of ethanol on soot reduction in our flames with that of laminar diffusion flames of gasoline and its surrogates in the literature [4,7] as shown in Fig. 7. Overall, ethanol presents a soot reduction effect in turbulent and laminar flames. The trend of soot reduction is very similar. However, the effect of soot reduction in the turbulent regime is stronger than that in the laminar regime. This is evident when comparing the evolution of soot reduction between the turbulent regime (blue filled circle) and the laminar regime (red circle) in the case of constant MFR. Only 2.75% carbon mass flow rate is reduced when 85% ethanol in volume is substituted in the TRF mixture (Table S2) by keeping constant FPW. Thus, the carbon mass flow rate of the initial mixture could be considered nearly constant in this case. It is possible to compare the evolution of the soot reduction between the turbulent regime with constant FPW (blue filled square) and the laminar regime with constant carbon mass flow rate (green diamond or green triangle). The soot reduction in the turbulent regime is always stronger than that in the laminar regime for the last comparison. This is an interesting point, which merits further investigations in the future with considering also possible influence of fuel spray characteristics.

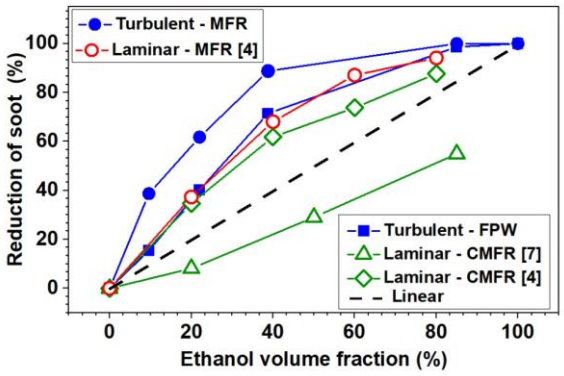

Fig. 7. Comparison of the reduction of the maximum soot volume fraction between the turbulent and the laminar regime in the TRF-Ethanol flames. MFR: constant fuel mass flow rate, FPW: constant flame power, CMFR: constant carbon mass flow rate.

3.3. Comparison between surrogate and real fuel E10

The proposition of a good surrogate is important and essential for fundamental and applied studies of real fuels. The combustion kinetics of gasoline surrogate have been investigated in the literature [22]. However, the combustion properties of a surrogate representing a gasoline/ethanol mixture has not been extensively investigated [7,12]. Thus, it is necessary to understand the combustion behavior of this kind of fuel before investigating the impact of ethanol on soot formation in a gasoline surrogate flame. In this section, we present the comparison between the E10 surrogate and E10 real fuel. Fig. 8 presents 2D-images of LII (a) and soot precursors from LIF (b) for 2 flames: TRF-E10 and E10 (constant FPW). We observed that the 2D plots of soot and soot precursors are nearly similar. The flame photographs are also similar as shown in the Fig. S5.

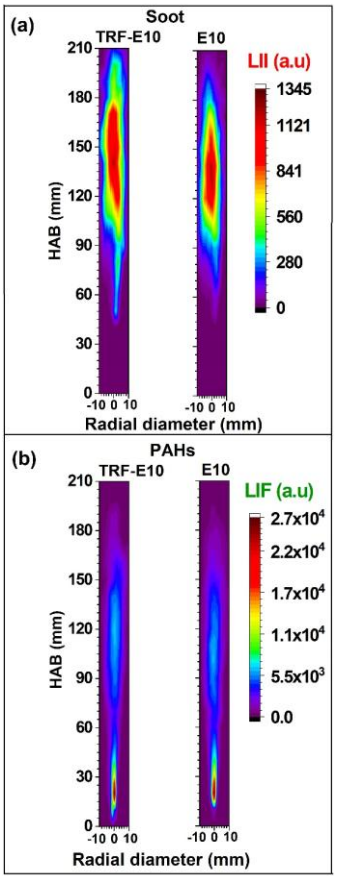

Fig. 8. 2D-images of LII (a) and soot precursors LIF (b) for 2 flames TRF-E10 and E10 (constant FPW).

Furthermore, Fig. 9 presents the profiles of temperature, pyrogenic PAHs and soot volume fraction obtained at the centerline of the two flames TRF-E10 and E10 respectively. The profile of temperature, pyrogenic PAHs, and soot volume fraction of TRF-E10 flame are quite similar to that of their corresponding real fuel E10. Similar results are also observed in the case of TRF-E85 and TRF-E10* flames as shown in Fig. S6,7,8,9. We do not present the comparison for the case of TRF-E85* flame because soot particles and their precursors were not detected in this flame. Thus, it can be concluded that the surrogates used in the present study are appropriate and well suited to investigate the impact of ethanol on the soot formation in the gasoline flame.

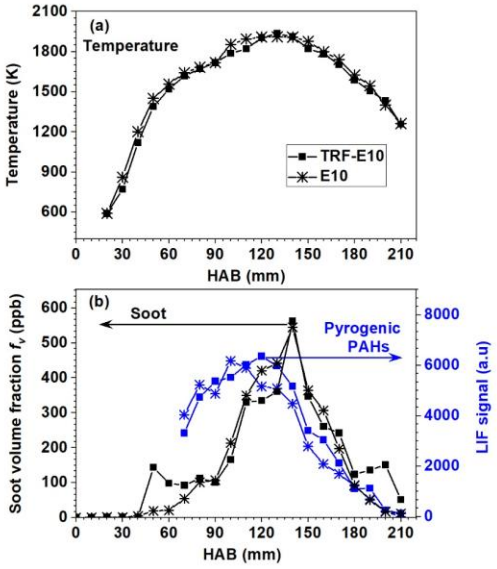

Fig. 9. Temperature profiles (a), pyrogenic PAHs and soot volume fraction profiles (b) obtained in flame TRF-E10 and E10 (constant FPW).

4. Conclusion

In this work, we carried out a series of experiments aiming to characterize the impact of ethanol on soot formation in different turbulent diffusion flames of gasoline and its surrogate. The obtained results providing a set of experimental data that bridges the gap between fundamental and applied studies of the two types, particularly those characterized by turbulent flames, are very limited in the literature. Two approaches have been carried out, i.e., by keeping the flame power constant or by keeping the mass flow rate of fuels constant. In both cases, we observed a reduction of soot volume fraction and pyrogenic PAHs in the TRF flame with increasing substituted ethanol but with a stronger efficiency for the case with constant MFR. Up to 40% ethanol, a quasi-linear reduction of the soot volume fraction was observed. After 40%, this trend is not respected, and from about 60 - 80% is sufficient to lead to ~100% soot reduction. Moreover, we also have an excellent agreement between the experiments carried out with commercial fuels E10, E10* and E85 and their corresponding surrogates which therefore validate the choice of these surrogates for soot formation studies from commercial fuels. We also showed that the centerline temperature profiles of all these flames exhibit similar maximum values. This indicates that the f_v reduction is mainly related to the chemical and dilution effect of ethanol, for which a modeling work will be soon performed to lead to a deeper understanding of the phenomenon. Moreover, the role of turbulence in the soot reduction efficiency when adding ethanol merits also further investigations.

Acknowledgements

This work was supported by the Agence Nationale de la Recherche through the OFELIE project (ANR-20-CE05-0047) and the LABEX CAPPA (ANR-11-LABX-0005). Financial and technical supports from the CERLA are also greatly appreciated.

Supplementary material (SM)

SM: Additional information (PDF file)

References

[1] L. Lešnik, B. Kegl, E. Torres-Jiménez, F. Cruz-Peragón, Why we should invest further in the development of internal combustion engines for road applications, Oil Gas Sci. Technol. – Rev. IFP Energies Nouvelles 75 (2020) 56.

[2] P. Dirrenberger, P.A. Glaude, R. Bounaceur, H. Le Gall, A.P. da Cruz, A.A. Konnov, F. Battin-Leclerc, Laminar burning velocity of gasolines with addition of ethanol, Fuel 115 (2014) 162–169.

[3] M.M. Maricq, J.J. Szente, K. Jahr, The Impact of Ethanol Fuel Blends on PM Emissions from a Light-Duty GDI Vehicle, Aerosol Science and Technology 46 (2012) 576–583.

[4] F. Liu, Y. Hua, H. Wu, C. Lee, X. He, An experimental study on soot distribution characteristics of ethanol-gasoline blends in laminar diffusion flames, Journal of the Energy Institute 91 (2018) 997–1008.

[5] F. Liu, Y. Hua, H. Wu, C. Lee, Y. Li, Experimental Investigation of Polycyclic Aromatic Hydrocarbons Growth Characteristics of Gasoline Mixed with Methanol, Ethanol, or n-Butanol in Laminar Diffusion Flames, Energy Fuels 32 (2018) 6823–6833.

[6] M. Matti Maricq, Soot formation in ethanol/gasoline fuel blend diffusion flames, Combustion and Flame 159 (2012) 170–180.
[7] A. Khosousi, F. Liu, S.B. Dworkin, N.A. Eaves, M.J. Thomson, X. He, Y. Dai, Y. Gao, F. Liu, S. Shuai, J. Wang, Experimental and numerical study of soot formation in laminar coflow diffusion flames of gasoline/ethanol blends, Combustion and Flame 162 (2015) 3925–3933.
[8] K.C. Kalvakala, P. Pal, G. Kukkadapu, M. McNenly, S. Aggarwal, Numerical Study of PAHs and Soot Emissions from Gasoline–Methanol, Gasoline–Ethanol, and Gasoline–n-Butanol Blend Surrogates, Energy Fuels 36 (2022) 7052–7064.
[9] K.C. Kalvakala, P. Pal, S.K. Aggarwal, Effects of fuel composition and octane sensitivity on polycyclic aromatic hydrocarbon and soot emissions of gasoline–ethanol blend surrogates, Combustion and Flame 221 (2020) 476–486.
[10] Y. Hua, X. Xiang, Y. Qian, S. Meng, B. Ye, Effect of diffusion oxygen enrichment on soot formation in coflow diffusion flames of gasoline-surrogate fuel doped with ethanol, Fuel 328 (2022) 125306.
[11] G. Jia, M. Yao, H. Liu, P. Zhang, B. Chen, L. Wei, PAHs formation simulation in the premixed laminar flames of TRF with alcohol addition using a semi-detailed combustion mechanism, Fuel 155 (2015) 44–54.
[12] R. Lemaire, E. Therssen, P. Desgroux, Effect of ethanol addition in gasoline and gasoline–surrogate on soot formation in turbulent spray flames, Fuel 89 (2010) 3952–3959.
[13] L. Xu, Y. Wang, D. Liu, Effects of oxygenated biofuel additives on soot formation: A comprehensive review of laboratory-scale studies, Fuel 313 (2022) 122635.
[14] R. Lemaire, M. Maugendre, T. Schuller, E. Therssen, J. Yon, Original use of a direct injection high efficiency nebulizer for the standardization of liquid fuels spray flames, Review of Scientific Instruments 80 (2009) 105105.
[15] J. Elias, A. Faccinetto, S. Batut, O. Carrivain, M. Sirignano, A. D'Anna, X. Mercier, Thermocouple-based thermometry for laminar sooting flames: Implementation of a fast and simple methodology, Int. J. Therm. Sci. 184 (2023) 107973.
[16] C. Betrancourt, F. Liu, P. Desgroux, X. Mercier, A. Faccinetto, M. Salamanca, L. Ruwe, K. Kohse-Höinghaus, D. Emmrich, A. Beyer, A. Gölzhäuser, T. Tritscher, Investigation of the size of the incandescent incipient soot particles in premixed sooting and nucleation flames of n-butane using LII, HIM, and 1 nm-SMPS, Aerosol Science and Technology 51 (2017) 916–935.
[17] C. Betrancourt, X. Mercier, F. Liu, P. Desgroux, Quantitative measurement of volume fraction profiles of soot of different maturities in premixed flames by extinction-calibrated laser-induced incandescence, Appl. Phys. B 125 (2019) 16.
[18] H.A. Michelsen, Effects of maturity and temperature on soot density and specific heat, Proceedings of the Combustion Institute 38 (2021) 1197–1205.
[19] C.K. Westbrook, W.J. Pitz, H.J. Curran, Chemical Kinetic Modeling Study of the Effects of Oxygenated Hydrocarbons on Soot Emissions from Diesel Engines, J. Phys. Chem. A 110 (2006) 6912–6922.
[20] T. Kim, J. Moon, J. Jeon, Characterization of in-cylinder spatiotemporal flame and solid particle emissions for ethanol-gasoline blended in gasoline direct injection engines, Energy 283 (2023) 128492.
[21] L. Chen, R. Stone, D. Richardson, A study of mixture preparation and PM emissions using a direct injection engine fuelled with stoichiometric gasoline/ethanol blends, Fuel 96 (2012) 120–130.
[22] H. Chu, L. Xiang, X. Nie, Y. Ya, M. Gu, J. E, Laminar burning velocity and pollutant emissions of the gasoline components and its surrogate fuels: A review, Fuel 269 (2020) 117451.